Available online at www.elixirpublishers.com (Elixir International Journal)

Mechanical Engineering

Elixir Mech. Engg. 52 (2012) 11638-11644

ISSN: 2229-712X

The effect of cooling rate on the microstructure and mechanical properties of Al-Si Alloy

P.A.O Adegbuyi, K.A. Adedeji, N.A Raji and A.O Akinbuja

Faculty of Engineering, Lagos State University, Ojo Lagos, P.M.B 1087, Apapa.Lagos, Nigeria.

ARTICLE INFO

Article history:

Received: 22 September 2012;

Received in revised form:

19 November 2012;

Accepted: 23 November 2012;

Keywords

Al-Si,

Cooling Rare,

Properties,

Effect.

ABSTRACT

This study focuses on a manufacturing process modification that can be carried out during the process of casting Aluminium-Silicon alloy in order to obtain desired properties and characteristics of a material for a particular usage. The effect of cooling rate was studied using sand and die moulds. Three types of mould were used namely dry sand mould, green sand mould and die mould .The result shows that the rate of cooling is faster in the die mould and the specimen obtained has the highest value of yield strength, ultimate tensile strength and hardness value but a low impact strength. The microstructure reveals that specimen A(dry sand mould) has a coarse microstructure, specimen B(green sand mould)exhibits a fairly wide spread distribution of silicon deposits while specimen C(die mould) exhibits fine and even distribution pf silicon deposits.

Introduction

It is a fact that all man-made structures are made from different variety of materials. Examples of these structures, ranging from the enormous ones, are buildings, bridges, ships, air-crafts e.t.c., down to the more compact & domestic ones; motorbikes, computer systems, cooking utensils e.t.c.

Specific materials are used for specific purposes due to quite a number of fundamental reasons. Safety, environment of application, cost, availability, internal and external characteristics of the material, to mention but a few, are part of these fundamental reasons. And it is because of the cautious consideration of these reasons that particular metals/alloys will be used in the construction of ships in place of any other metal/alloy, polymer or wood.

Out of all these reasons, “safety and cost” are primary, with safety taking the first spot between the two. In the general view of safety features like strength, durability, resistance to chemical effects amongst others are imperative things to consider in a material. And all these lies in the internal and external characteristics of a material. As for cost, this relates to the availability of the material, process of extraction of/producing the material, the process by which the material can be used in manufacturing products and so on.

Metals and their alloys compared to all other materials possess the needed characteristics for safety such as strength and others. But in using metals/alloys, the area of application must be considered. Non-abundance, cost limitation and other reasons affect the use of metals such as gold, silver, chromium e.t.c. in wider area of applications. It is because of these reasons that manufacturers find ways in bringing-out substitutes by modifying the characteristics of other metals to suit the purpose of application.

Aluminium is one of the major metals used in the manufacturing industries. It is used in the bringing-out of variety of products in industries such as food packaging, aircraft production, automobile production, marine field, construction and so on. Its usage has increased over the past 30 years at a fairly steady rate.

In recent times, materials / manufacturing process researchers have been carrying-out analytical tests in finding ways of improving the qualities of alloys made from aluminium in order for it to be used in more areas of application. For instance, in the automobile industry, work is been carried-out in producing aluminium-silicon alloy engine blocks which will eliminate the use of iron in producing engine blocks or using iron as liners in the engine cylinders.

In line with the above, this work focuses on a manufacturing process modification that can be carried-out during the casting of aluminium-silicon alloy in producing. components that will have the necessary characteristics desired in their respective areas usage

Experimental methods

For this research work, an aluminium-silicon alloy which falls between the hypo- and hyper-eutectic transition range was used. This is so because the silicon content in the alloy is about 12%. This alloy was prepared by adding 58g of ferro-silicon (80% silicon content) to 400g of Al 6063 alloy. The Al 6063 was purchased from Nigerian Aluminium Extrusion Company (Nigalex), Oshodi.

Table 1. Chemical Analysis Of Al 6063

Al	Si	Fe	Cu	Mn	Mg	Zn	Cr	Ti	Ca	Sr
98.5 36	0.4 75	0.3 11	0.0 33	0.0 35	0.5 31	0.0 39	0.0 07	0.0 06	0.00 01	0.0 01

(i) Dry sand mould - SPECIMEN A

(ii) Green sand mould - SPECIMEN B

(iii) Die mould - SPECIMEN C

And also a control specimen (for base reference) was made from Al6063 alloy using the die mould - CONTROL SPECIMEN

The moulds for the specimens were put in order, after which the alloy was prepared in a crucible furnace. The crucible

Tele:

E-mail addresses: paorene011@yahoo.com

furnace used is shown below in Fig. 2.1 The preparation of the alloy in the furnace has to do with heating-up the Al 6063 alloy to its molten state and adding the ferro-silicon to it in order to cast specimens A, B and C. But for the control specimen the Al 6063 alloy was melted separately without the addition of ferro-silicon.

Fig. 2.1. Crucible furnace

The alloy was allowed to melt and stay in its molten form until the temperature read 710^0C. At this stage, the alloy was poured into each mould. The time taken for the alloy to solidify and cool down to a temperature of about 37^0C was noted down for each mould. This enabled the calculation of the cooling rate of each mould as shown in Table 2.1 below.

Table 2.1 The Cooling Rate Of The Moulds Used In The Casting Process

SPECIMEN	MOULD	POURING TEMPERATURE	COOLING TIME TO 37^0C (Seconds)	COOLING RATE ($^0Cs^{-1}$)
A	DRY SAND	710^0C	4320	0.156
B	GREEN SAND	710^0C	4200	0.160
C	DIE	710^0C	3540	0.190
CONTROL	DIE	710^0C	3600	0.187

Fig. 2.2. Cast specimens

Fig. 2.3. Fractured specimen after loading

Discussion of results and conclusion

This work is focused on the manner by which the microstructure and mechanical properties of an Aluminium-Silicon cast alloy will be altered by variation in the cooling rate of the moulds used in the casting process.

From the experimental work carried-out and results obtained, observations were made and necessary tables and graphs where drawn-out. Also, a comparison table of all results was prepared as shown below in Table 3.1

From the above table, it can be seen that the inclusion of about 12% silicon into the AI6063 alloy causes:

1. noticeable increment in the ultimate tensile strength (UTS) of the die cast specimen but reduction in that of both the dry and green sand cast specimens.
2. reduction in the yield strength of all the specimen (i.e. A, B and C).
3. reduction in the hardness number of all the specimens (i.e. A, B and C).
4. increment in the impact strength (toughness) of all the specimens (i.e. A, B and C)

The rate of cooling as shown in table 3.1 implies that the die mould specimen cools faster compared to the sand (dry and green) mould specimens. The resultant effect this has on the mechanical properties is that:

1. The die mould cast (specimen C) has the highest value for yield strength, ultimate tensile strength and hardness number compared to the dry and green sand casts (Specimen A and B)
2. The impact strength (toughness) of specimen C is the lowest compared to specimen A and B.

As for the cooling rate effect on the microstructures of each specimen, it was discovered that:

1. the micrograph of specimen A (Fig. 3.1) depicts uneven (localized distribution of silicon deposits and a large grain size structure due to the continuous growth of grains before complete solidification this is as a result of slow cooling effect. It can be simply stated that specimen A has a coarse microstructure.
2. the micrograph of specimen B (fig. 3.2) depicts fairly widespread distribution of the silicon deposits. Compared with the micrograph of specimen A, specimen B has a little bit more grains per unit area but the grain sizes are big. The causes of this is linked to the rate of cooling being a bit faster than that of specimen A.
3. the micrograph of specimen C (Fig. 3.3) shows a fine and even distribution of silicon deposits. The grain sizes are small and the direction of arrangement is along a particular path. This is as a result of the rapid cooling which hinders excessive growth of grains during solidification.

On a concluding note, it can be said that the castings made from sand moulds generally cool slowly. And this increases the casting's grain size, creating a coarse microstructure that lowers the strength of the casting. Coarse grains can allow elements of an alloy to separate, which also weakens the casting. But slow cooling keeps the casting metal liquid longer, which allows more gases and waste metal to escape, reducing the voids and inclusions that can weaken a casting.

Conversely, casting made from die moulds generally cool more quickly, resulting in a fine microstructure with small-sized grains and less alloy segregation. This increases the strength of the casting. But fast cooling allows quick solidification of casting metal liquid thereby allowing gases to be trapped inside the casting.

Table 3. A comparison table of all results

SPECIMEN (BASE ALLOY A16063)	MOULD USED	COOLIN GRATE ($^{O}C_{S}^{-1}$)	YIELD STRENGHT H (MPa)	ULTIMATE TENSILE STRENGTH (MPa)	HARDNESS NUMBER	IMPACT NUMBER (mkg)
A (+12%Silicon)	DRY SAND	0.156	33.93180	146.6449415	71.2	1.078
B (+12%Silicon)	GREEN SAND	0.160	46.04910	135.0185459	73.1	0.968
C (+12%Silicon)	DIE	0.190	46.06810	202.0590439	74.0	0.899
CONTROL (AI6063)	DIE	0.187	55.92523	180.1523031	74.8	0.857

Appendix

Table 4.3a. Results from tensile test {control specimen (al 6063)}

	Diameter (mm)	Area (cm^2)	Load at Break (Standard) (N)	Extension at Break (Standard) (mm)
1	5.80000	0.26421	4759.80379	3.51656

	Tensile stress at Break (Standard) (MPa)	Tensile strain at Break (Standard) (mm/mm)	Tensile stress at Yield (Zero Slope) (MPa)	Modulus (Automatic) (MPa)
1	180.15370	0.12093	55.92523	3957.06017

	Energy at Break (Standard) (J)	Energy at Yield (Zero Slope) (J)	Extension at Yield (Zero Slope) (mm)	Load at Yield (Zero Slope) (N)
1	8.15646	8.15646	3.51656	4759.80379

	Tensile strain at Yield (Zero Slope) (mm/mm)	Poisson's Ratio (Chord)	Energy to X-Intercept at Modulus (Automatic) (J)	True strain at Yield (Zero Slope) (mm/mm)
1	0.12093	-----	0.01781	0.11416

	True stress at Yield (Zero Slope) (Pa)	Specimen Label	Length (mm)
1	201939178.17498	Control	29.08000

Table 4.3b. Tensile test table for control specimen (al 6063)

TIME (sec)	EXTENSION (mm)	LOAD (N)	ENGRG STRAIN %	ENGRG STRESS (Mpa)	TRUE STRESS (Mpa)	TRUE STRAIN %
0	0	0.4339179	0	0.01642322	0.01642322	0
1	0.1665625	13.4168	0.572773384	0.507808183	0.798667194	0.452840547
2	0.3331249	14.28489	1.145546424	0.540664244	1.160020236	0.763394263
3	0.4999999	14.59486	1.719394429	0.5523962	1.502183149	1.000409219
4	0.6668749	39.10117	2.293242435	1.479927709	4.873760732	1.191872622
5	0.8331249	215.1106	2.864941197	8.141652473	31.46700805	1.351946468
6	0.9996874	840.2294	3.43771458	31.80157451	141.1263109	1.49013951
7	1.166562	1477.357	4.01156121	55.91601378	280.2265257	1.611747485
8	1.333125	1925.015	4.584336314	72.8592786	406.8707153	1.719965592
9	1.500156	2209.715	5.15872077	83.63479808	515.083368	1.817869089
10	1.666719	2419.247	5.731495873	91.5653079	616.3714923	1.906797388
11	1.833125	2625.126	6.303731087	99.35755649	725.680874	1.988385325
12	2	2869.246	6.877579092	108.5971765	855.482847	2.064020635
13	2.166718	3124.395	7.450887208	118.2542296	999.3531561	2.134271431
14	2.333593	3379.426	8.024735213	127.9068165	1154.325151	2.199969165
15	2.499843	3625.283	8.596433975	137.2121797	1316.747623	2.261391569
16	2.666562	3859.454	9.16974553	146.0752432	1485.548051	2.319417188
17	2.832968	4075.401	9.741980743	154.2485523	1656.934978	2.374159499
18	3.000156	4277.286	10.31690509	161.8896332	1832.089614	2.426297633
19	3.166718	4458.1	10.88967675	168.7332046	2006.183261	2.475670524
20	3.333125	4619.799	11.46191541	174.8532985	2179.007014	2.522677226
21	3.499687	4751.836	12.03468707	179.8507248	2344.297917	2.56761404
21.1	3.516562	4759.804	12.09271664	180.1523031	2358.683057	2.572056094
21.192	3.534531	2687.542	12.15450825	101.7199198	1338.075524	2.576764533

Table 4.4a. Results from tensile test (specimen a)

	Diameter (mm)	Area (cm^2)	Load at Break (Standard) (N)	Extension at Break (Standard) (mm)
1	5.80000	0.26421	3874.50643	3.50000

	Tensile stress at Break (Standard) (MPa)	Tensile strain at Break (Standard) (mm/mm)	Tensile stress at Yield (Zero Slope) (MPa)	Modulus (Automatic) (MPa)
1	146.64610	0.12036	33.93180	731.02596

	Energy at Break (Standard) (J)	Energy at Yield (Zero Slope) (J)	Extension at Yield (Zero Slope) (mm)	Load at Yield (Zero Slope) (N)
1	5.63149	0.01504	0.18328	113.32443

	Tensile strain at Yield (Zero Slope) (mm/mm)	Poisson's Ratio (Chord)	Energy to X-Intercept at Modulus (Automatic) (J)	True strain at Yield (Zero Slope) (mm/mm)
1	0.00630	-----	-----	0.00628

	True stress at Yield (Zero Slope) (Pa)	Specimen Label	Length (mm)
1	4316246.93125	A	29.08000

Table 4.4b. Tensile Test Table For Specimen A

TIME (sec)	EXTENSION (mm)	LOAD (N)	ENGRG STRAIN %	ENGRG STRESS (Mpa)	TRUE STRESS (Mpa)	TRUE STRAIN %
0	0	0.04918193	0	0.001861471	0.001861471	0
1	0.166875	112.2665	0.573848006	4.249138943	6.68749885	0.45352358
2	0.3332812	112.3046	1.146083906	4.250580977	9.122103428	0.763644742
3	0.4999999	112.5949	1.719394429	4.261568449	11.5888855	1.000409219
4	0.6667186	112.8877	2.292704952	4.272650543	14.0685776	1.191709401
5	0.8332811	148.9037	2.865478336	5.635808637	21.78509619	1.352085435
6	0.9999998	314.0939	3.438788858	11.88803982	52.76849869	1.49038156
7	1.166562	896.3	4.01156121	33.92377276	170.0110637	1.611747485
8	1.333125	1205.762	4.584336314	45.63650127	254.8495713	1.719965592
9	1.499844	1402.781	5.157647868	53.09341054	326.9305262	1.817694865
10	1.666562	1556.388	5.730955983	58.90723288	396.5019916	1.906717182
11	1.833437	1716.046	6.304803989	64.95007759	474.4475859	1.988532212
12	1.999843	1847.784	6.877039202	69.93618712	550.8900876	2.063952098
13	2.166562	1986.074	7.450350757	75.17028122	635.2152427	2.13420795
14	2.333125	2168.483	8.02312586	82.07422126	740.5660283	2.199790822
15	2.500312	2390.265	8.598046768	90.46837743	868.3197175	2.261559616
16	2.666718	2634.836	9.170281981	99.72506718	1014.232054	2.319469936
17	2.833437	2898.906	9.743593535	109.7197684	1178.784594	2.374309627
18	2.999843	3154.309	10.31582875	119.386435	1350.956454	2.42620252
19	3.166718	3404.855	10.88967675	128.8692707	1532.213972	2.475670524
20	3.333281	3647.676	11.46245186	138.0597252	1720.562679	2.522720272
21	3.5	3874.506	12.03576341	146.6449415	1911.628763	2.567696612
21.072	3.513906	2211.397	12.08358322	83.69845956	1095.075761	2.571358255

Table 4.5A. Results From Tensile Test (Specimen B)

	Diameter (mm)	Area (cm^2)	Load at Break (Standard) (N)	Extension at Break (Standard) (mm)
1	5.80000	0.26421	3567.32532	3.18297

	Tensile stress at Break (Standard) (MPa)	Tensile strain at Break (Standard) (mm/mm)	Tensile stress at Yield (Zero Slope) (MPa)	Modulus (Automatic) (MPa)
1	135.01961	0.10946	46.04910	3540.54888

	Energy at Break (Standard) (J)	Energy at Yield (Zero Slope) (J)	Extension at Yield (Zero Slope) (mm)	Load at Yield (Zero Slope) (N)
1	4.86514	4.86514	3.18297	3567.32532

	Tensile strain at Yield (Zero Slope) (mm/mm)	Poisson's Ratio (Chord)	Energy to X-Intercept at Modulus (Automatic) (J)	True strain at Yield (Zero Slope) (mm/mm)
1	0.10946	-----	0.00718	0.10387

	True stress at Yield (Zero Slope) (Pa)	Specimen Label	Length (mm)
1	149798262.39989	B	29.08000

Table 4.5b. Tensile test table for specimen b

TIME (sec)	EXTENSION (mm)	LOAD (N)	ENGRG STRAIN %	ENGRG STRESS (Mpa)	TRUE STRESS (Mpa)	TRUE STRAIN %
0	0	0.387039	0	0.014648916	0.014648916	0
1	0.1670312	2.764052	0.574385144	0.104615722	0.164705439	0.453864812
2	0.3335937	3.638418	1.147158528	0.137709322	0.295683745	0.764145353
3	0.4996874	3.301695	1.718319807	0.124964801	0.339694293	1.000013972
4	0.6665624	8.000425	2.292167813	0.302805533	0.996886631	1.191546257
5	0.8332811	147.9233	2.865478336	5.59870179	21.64166048	1.352085435
6	0.9999998	748.7979	3.438788858	28.34101283	125.799772	1.49038156
7	1.166875	1216.641	4.012637552	46.04825707	230.8232226	1.611962234
8	1.333125	1421.434	4.584336314	53.79940199	300.4339542	1.719965592
9	1.499687	1559.266	5.157107978	59.01616139	363.3688781	1.817607183
10	1.666562	1660.017	5.730955983	62.82945384	422.9022883	1.906717182
11	1.83375	1788.331	6.30588033	67.68596949	494.5055932	1.988679549
12	2	1972.551	6.877579092	74.6584535	588.1278724	2.064020635
13	2.166562	2181.315	7.450350757	82.55989554	697.6600757	2.13420795
14	2.333125	2399.808	8.02312586	90.82956739	819.5666183	2.199790822
15	2.499999	2630.182	8.596970426	99.54891942	955.3680357	2.261447468
16	2.667031	2871.084	9.171358322	108.6667424	1105.288374	2.319575763
17	2.833593	3109.183	9.744129986	117.6784755	1264.352837	2.374359558
18	2.999687	3336.627	10.3152923	126.2869309	1428.973536	2.426155111
19	3.166562	3547.95	10.8891403	134.2852277	1596.535912	2.475625404
19.1	3.182968	3567.325	10.94555708	135.0185459	1612.871747	2.480359417
19.19	3.200156	1983.766	11.004663	75.08292646	901.3452291	2.485295158

Table 4.6a. Results From Tensile Test (Specimen C)

	Diameter (mm)	Area (cm^2)	Load at Break (Standard) (N)	Extension at Break (Standard) (mm)
1	5.80000	0.26421	5338.60177	4.85000

	Tensile stress at Break (Standard) (MPa)	Tensile strain at Break (Standard) (mm/mm)	Tensile stress at Yield (Zero Slope) (MPa)	Modulus (Automatic) (MPa)
1	202.06061	0.16678	46.06810	3422.38544

	Energy at Break (Standard) (J)	Energy at Yield (Zero Slope) (J)	Extension at Yield (Zero Slope) (mm)	Load at Yield (Zero Slope) (N)
1	10.72798	0.46100	1.33328	1217.15581

	Tensile strain at Yield (Zero Slope) (mm/mm)	Poisson's Ratio (Chord)	Energy to X-Intercept at Modulus (Automatic) (J)	True strain at Yield (Zero Slope) (mm/mm)
1	0.04585	-----	0.08498	0.04483

	True stress at Yield (Zero Slope) (Pa)	Specimen Label	Length (mm)
1	48180265.47616	Aluminium Alloy	29.08000

Table 4.6b. Tensile Test Table For Specimen C

TIME (sec)	EXTENSION (mm)	LOAD (N)	ENGRG STRAIN %	ENGRG STRESS (Mpa)	TRUE STRESS (Mpa)	TRUE STRAIN %
0	0	0.1265682	0	0.004790439	0.004790439	0
1	0.1667187	98.94028	0.573310523	3.744759093	5.891668886	0.453182013
2	0.3331249	98.76502	1.145546424	3.738125733	8.020322298	0.763394263
3	0.4998437	99.05488	1.71885729	3.749096552	10.19325849	1.000211678
4	0.6665624	100.5737	2.292167813	3.806581886	12.53190636	1.191546257
5	0.8332811	216.7265	2.865478336	8.202812157	31.70779268	1.352085435
6	0.9999998	511.3923	3.438788858	19.35552401	85.91508434	1.49038156
7	1.166562	1022.562	4.01156121	38.70262291	193.9605637	1.611747485
8	1.333281	1217.156	4.584872765	46.06774914	257.2825175	1.720061651
9	1.499844	1116.617	5.157647868	42.2624806	260.2374736	1.817694865
10	1.667031	1174.17	5.732568776	44.44078574	299.2006464	1.906956761
11	1.833281	1308.724	6.304267538	49.53347716	361.8057692	1.988458772
12	2	1475.067	6.877579092	55.8293403	439.8000439	2.064020635
13	2.166718	1667.85	7.450887208	63.12592256	533.4700515	2.134271431
14	2.333437	1881.535	8.024198762	71.21361796	642.645843	2.19990972
15	2.499999	2096.13	8.596970426	79.33575565	761.3829007	2.261447468
16	2.666718	2297.106	9.170281981	86.94243216	884.2290511	2.319469936
17	2.833124	2487.417	9.742517194	94.14545248	1011.359142	2.374209437
18	2.999843	2655.877	10.31582875	100.5214413	1137.483415	2.42620252
19	3.166562	2846.399	10.8891403	107.7324477	1280.846186	2.475625404
20	3.333281	3056.497	11.46245186	115.6843798	1441.711014	2.522720272
29	4.833437	5320.447	16.62117263	201.3719011	3548.409032	2.869101169
29.1	4.849999	5338.602	16.67812586	202.0590439	3572.02521	2.872328048
29.188	4.867499	2991.508	16.73830468	113.2246319	2008.413018	2.875726407

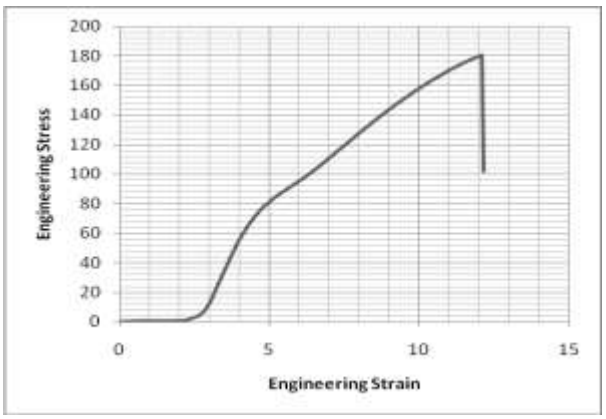

Fig. 4.2. Graph of engineering stress against strain (control specimen)

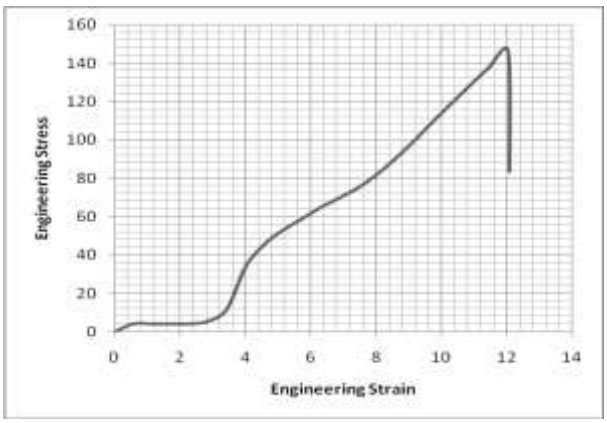

Fig. 4.3. Graph of engineering stress against strain (specimen A)

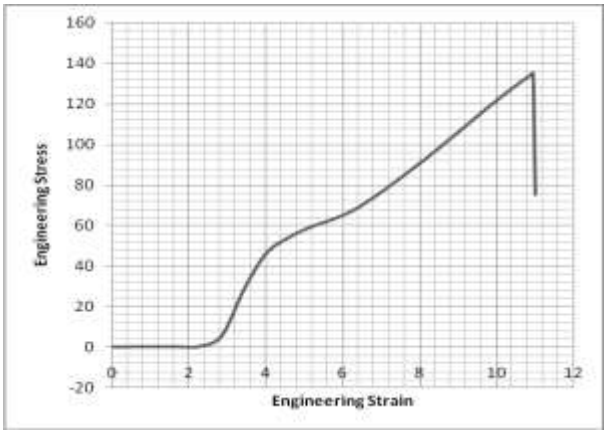

Fig. 4.4. Graph of engineering stress against strain (specimen B)

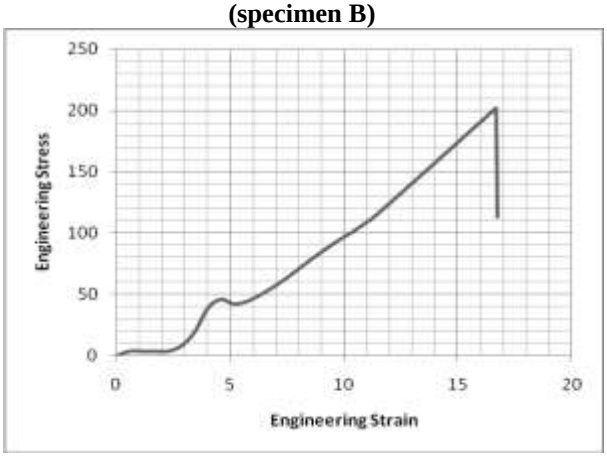

Fig. 4.5. Graph of engineering stress against strain (specimen C)

Hardness Test

The Vicker's hardness test was used for this work and the results obtained are shown in table 4.7 below.

Table 4.7. Hardness number for each specimen

Specification	Hardness test
CONTROL	74.8
SPECIMEN A	71.2
SPECIMEN B	73.1
SPECIMEN C	74.0

Impact Test

Impact load in producing stress depends on the extent to which the energy is expended in causing deformation.

The results obtained from the impact test are shown in Table 4.8 below.

Table 4.8. Impact test values for each specimen

Specification	Impact Test [m.kg]
CONTROL	0.857
SPECIMEN A	1.078
SPECIMEN B	0.968
SPECIMEN C	0.899

Fig. 3.1. Micrograph of specimen a (magnification: 10X)

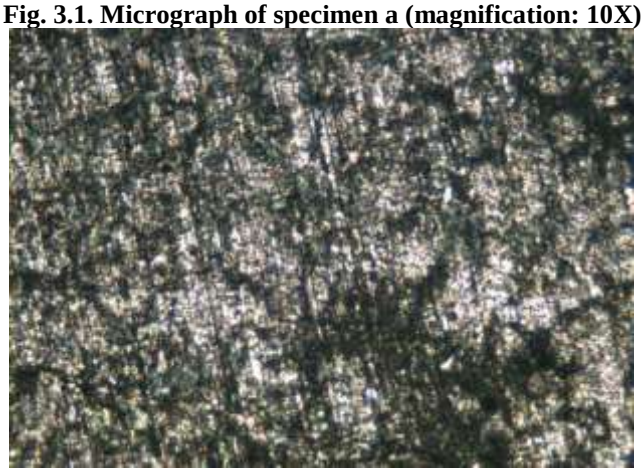

Fig. 3.2. Micrograph of specimen b (magnification: 10X)

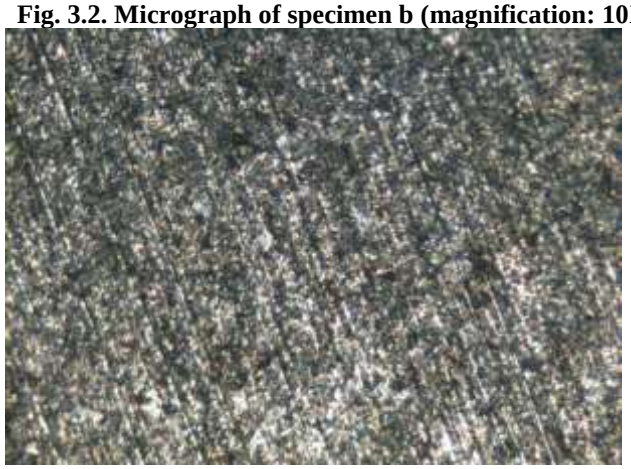

Fig. 3.3. Micrograph of specimen c (magnification: 10X)

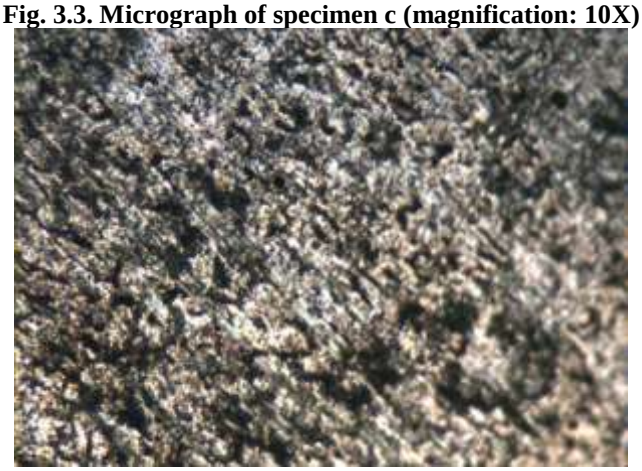

Fig. 3.4. Micrograph of control specimen (magnification: 10X)

References

1. J PATHAK and S. MOHAN," Tribological behavior of conventional Al–Sn and equivalent Al–Pb alloys under lubrication" Bull. Mater. Sci., Vol. 26, No. 3, April 2003.
2. ASM Metals Handbook ,"Casting', Volume 15 of the 9th Edition,1992.
3. P. Groover ,"Fundemental of modern manufacturing'', Materials , Processes,Systems,2007.
4.Y. Rihan," Numerical study on the effect of solidification Parameters during the continuous casting of Al-Si alloys", the Online Journal on Mathematics and Statistics (OJMS) Vol. 1 No. 1,2010.
5. D. Schmidt," Solid cast, effective casting simulation, solidification Time"2010.
6. S.Hurst," Metal casting", Intermediate Technology Publications 1996.
7. R. Askeland, "The Science and Engineering of Materials, 4th Edition,
8. S.Kalpakjian, "Manufaturing processes for engineering materials", Fifth Edition,2008.
9. B. Cantor ,"Solidification and casting", Series in Materials Science and Engineering,2003.
10. B. Rundman," Metal casting",2003.
11. J.Campbell," Castings, The new metallurgy of cast metals", Second Edition,2003.
12. M. El Rayes," Prediction of solidification time: chvorinov's rule",2007.
13. E. Michael Wagih , E. Khalil "Effect of volume and surface area on the total solidification time of metals & microstructure", The American university in Cairo.
14. M. Okazaki, J. Takahashi," Estimation of solidification time during casting by use of a heat transfer model", Journal of dental research.
15. B. Varaga, Metalurgica international, vol. XV, No. 8 (2010).
16. Mattia," Correlation between micro structural and mechanical properties of Aluminum alloy castings produced by different foundry processes",2008.
17. G.T. Abdel-Jaber and A. M. Omran,'' An Investigation into solidification and mechanical properties behavior of Al- Si casting alloys'', International Journal of Mechanical & Mechatronics Engineering IJMME-IJENS Vol: 10 No: 1
18 H. Yamagata, W. Kasprzak, M. Aniolek, H. Kurita, J.H. Sokolowski, The effect of average cooling rates on the microstructure of the Al–20% Si high pressure die casting alloy used for monolithic cylinder blocks, Journal of Materials Processing Technology 203/1-3 (2008) 333-341
19. M. Kasprzak, W. Kasprzak, J.H. Sokolowski, Applications of the Universal Metallurgical Simulator and Analyzer (UMSA) for the Physical Simulation of Industrial Light Metals Castings Processes, Proceedings of the International Conference "Technology Transfer Partnership for the Development of the Aluminium Industry", Montreal, 2002.
20. M. Krupi□ski, K. Labisz, L.A. Dobrza□ski, Structure investigation of the Al-Si-Cu alloy using derivative thermo analysis, Journal of Achievements in Materials and Manufacturing Engineering 34/1 (2009) 47-54
21. M. Krupi□ski, K. Labisz, L.A. Dobrza□ski, Z.M. Rdzawski, Derivative thermo-analysis application to assess the cooling rate influence on the microstructure of Al-Si alloy cast, Journal of Achievements in Materials and Manufacturing Engineering 38/2 (2010) 115-122
22. G. Pelayo, J.H. Sokolowski, R. Lashkari, A case based reasoning aluminum thermal analysis platform for the prediction of W319 Al cast component characteristics, Journal of Achievements in Materials and Manufacturing Engineering 36/1 (2009) 7-17.